



Essential secondary metabolites of *Azadirachta indica* leaf in search of drug for COVID-19 treatment: *In-silico* ADMET and bioactivity predictions

Paul Chijioke OZIOKO^{1*}, Daniel Danladi GAIYA¹ and Idris ABDULLAHI²

¹Biology Unit, Faculty of Science, Air Force Institute of Technology (AFIT) Kaduna, Kaduna State, Nigeria.

(E-mail: gaiyadaniel@gmail.com, +2348138348841)

²Department of Pharmaceutical and Medicinal Chemistry, Faculty of Pharmaceutical Sciences, Kaduna State University, Kaduna, Nigeria.

(E-mail: idrisabdulkd@gmail.com, +2348033543430)

*Corresponding Author: (+2347035310598; E-mail: paulcj82@gmail.com; LiveDNA: 234.37555)

Abstract

Introduction: A pandemic of acute respiratory sickness known as "coronavirus disease 2019" has been triggered by the highly transmissible and dangerous coronavirus, SARS-CoV-2, which poses risks to both public health and safety. The ADMET and bioactive properties of bioactive metabolites of *A. indica* leaf were predicted in the search for potential drug(s) for treatment and management of COVID-19. **Research Method:** The pharmacokinetic properties of 12 secondary metabolites from *A. indica* and 5 FDA approved drugs for treatment of COVID-19 were predicted using SWISSADME and ADMETlab online tools and Molinspiration server for bioactivity prediction. **Results:** The bioactive secondary metabolites and the drugs showed good ADMET and bioactivity properties, but ivermectin, azadirachtin A, azadirachtin D, azadirachtin H, azadirachtin F, azadirachtin I and nimbolin, have relatively poor properties. Similarly, most of the compounds have relatively tolerable toxicity level but remdesivir and nimboline. However, compounds from *A. indica* showed better properties in comparison to the FDA approved drug for COVID-19 treatment. **Conclusion:** Some of these compounds from *A. indica* leaf have relatively good ADMET and bioactive properties, and hence the need to dock them with human ACE2 in order to evaluate their binding interactions and thus their respective inhibitory constants.

Keywords: ADMET, *A. indica*, COVID-19, secondary metabolites, SARS-CoV-2, bioactivity and pharmacokinetic.

1.0 Introduction

The acute respiratory disease coronavirus disease 2019 (also known as COVID-19) (ICTV 2020) is a pandemic that presents dangers to both public health and safety. The highly contagious and pathogenic SARS-CoV-2 coronavirus, which first surfaced in late 2019, was the culprit. According to Mehta *et al.* (2020), positive-sense single-stranded RNA coronavirus 2 is linked to severe acute respiratory syndrome. Even though it is less deadly than the Middle East respiratory syndrome coronavirus (MERS-CoV) and severe acute respiratory syndrome coronavirus (SARS-CoV), the rapid spread of this highly contagious sickness has posed the greatest threat to global health in this century (Hu *et al.*, 2021). It is the third human coronavirus known to utilize the peptidase, angiotensin converting enzyme 2 (ACE2), to penetrate hosts, after SARS-CoV and MERS-CoV. SARS-CoV-2 and ACE2's interaction is crucial for the development of COVID-19 from an early infection to a severe sickness. Understanding the cellular origins of SARS-CoV-2 infection may help researchers develop treatments that stop the onset of severe sickness and, as a result, reduce mortality.

Three of the seven known human coronaviruses—SARS-CoV, SARS-CoV-2, and MERS-CoV—are extremely pathogenic, while the other four—HCoV-NL63, HCoV-229E, HCoV-OC43, and HCoV-HKU1—cause "common colds" and are less virulent. The ACE2 is the receptor used by SARS-CoV, SARS-CoV-2, and HCoV-NL63 to enter cells. According to Zhou *et al.* (2020), HCoV-229E utilizes CD13 (aminopeptidase N), whereas MERS-CoV binds DPP-4 (dipeptidyl peptidase-4). Given that the interactions do not necessitate the endopeptidase active site, it appears to be a major coincidence that all known human coronavirus receptors are cell surface peptidases. The fact that three coronaviruses have been selected to attack a specific region of ACE2 is noteworthy (Zhou *et al.*, 2020; Hoffmann *et al.*, 2020). Contrarily, the receptor-binding domain of the spike (S) protein is encoded by the coronavirus genome's most variable region. This

indicates that several sequences using varied structural strategies converging on the same region of the same protein were created by the diversity of these viruses.

Despite some treatments having shown some promise in certain patient subpopulations or for certain objectives, antivirals against SARS-CoV-2 and COVID-19 have not yet been proven to be generally effective treatments. SARS-CoV-2 is activated to enter the cell via human proteases acting as entry activators, while ACE2 acts as the receptor for the virus. Therefore, COVID-19 could be treated with medications that block this entry. Therefore, a potential therapeutic strategy is to prevent the S protein from binding to ACE2 by using soluble recombinant hACE2, specific monoclonal antibodies, or fusion inhibitors that target the SARS-CoV-2 S protein (Monteil *et al.*, 2020; Tian *et al.*, 2020; Xia *et al.*, 2020). Therefore, screening medicinal plants that contain a wide variety of bioactive chemical repositories may be a good first step in identifying possible therapeutic candidates for treating SARS-CoV-2. As a result, this study looked into the *in-silico* pharmacokinetic properties of secondary metabolites from *A. indica* leaf.

According to Prashanth and Krishnaiah (2014), *Azadirachta indica* Linn is a tropical evergreen tree that is native to India and is also present in other Southeast Asian countries. Locals call it "Neem," and it is a member of the Meliaceae mahogany family. This important medicinal plant, which has been dubbed the "Tree of the 21st Century" by the UN, has historically been used to treat a number of illnesses. It is called "Divine Tree," "Life Giving Tree," "Nature's Drugstore," "Village Pharmacy," and "Panacea for All Diseases" in India, according to Hossain and Nagooru (2011) and Ghimeray *et al.* (2009). In tropical and subtropical climates, including Nigeria, it thrives. According to studies (El-Hawary *et al.*, 2013; Pandey *et al.*, 2012), the bitter compounds found in almost every part of the neem tree—fruit, seeds, oil, leaves, roots, and bark—have antiviral, anti-retroviral, anti-inflammatory, anti-ulcer, anti-fungal,

antibacterial, anti-plasmodial, antiseptic, antipyretic, and anti-diabetic properties. Ascorbic acid, n-hexacosanol, amino acids, 7-desacetyl-7-benzoylazadiradione, 7-desacetyl-7-benzoylgedunin, 17-hydroxyazadiradione, and nimbiol are among the chemical components that can be found in neem leaves (Hossaina *et al.*, 2013). Some of the other primary active components include nimbolin, nimbin, nimbidin, nimbidol, sodium nimbinat, gedunin, salannin, and quercetin (Biswas *et al.*, 2002). The most important active component, azadirachtin, is also well known for its biological activity and medicinal properties. It is possible to computationally screen the pharmacokinetic characteristics of its bioactive elements in advance to assess their antiviral effectiveness in the treatment of the virulent and globally endemic COVID-19 virus. The reason for this is because the leaves have a wide range of biological and therapeutic qualities (El-Hawary *et al.*, 2013; Pandey *et al.*, 2012; Britto and Sheeba, 2011). Recently, it was discovered that the bioactive secondary metabolite azadirachtin-A from *A. indica* may be able to block the main protease of the SARS-CoV-2 virus (Muhammed *et al.*, 2021; Borkotoky and Banerjee, 2020; Fernandes *et al.*, 2019). Therefore, the goal of this study was to estimate the *in-silico* ADMET and bioactivity of key bioactive chemicals from *A. indica* leaf that may have possible inhibitory effects on human ACE2, which is crucial for COVID-19 entrance and invasion into host cells.

2.0 Materials and Methods

2.1 Ligands/Metabolites Selection:

In the works of Loganathan *et al.* (2021) and Mohammad and Forough (2007), unique and essential secondary metabolites (ligands) were identified from the leaf of *A. indica*, and their two-dimensional (2-D) structures were downloaded and retrieved from the PubChem database (Kim *et al.* 2016). PubChem (<https://pubchem.ncbi.nlm.nih.gov>) has one of the largest databases of publicly available chemical information and has rapidly developed into a key chemical information resource, serving scientific

communities in a variety of fields including cheminformatics, chemical biology, medicinal chemistry, and drug discovery (Kim *et al.* 2016).

The compounds or ligands chosen were: Azadirachtin-A, Azadirachtin-D, Azadirachtin-H, Azadirachtin-F, Azadirachtin-I, Desacetylnimbin, Azadiradione, Nimbin, Nimbolin, Nimbolide, Nimbinene, and Azadirone.

Some US Food and Drug Administration (FDA)-approved drugs for the treatment of COVID-19 were equally included. Remdesivir, Baricitinib, Paritaprevir, Ivermectin, and 2-monolinolenin were equally retrieved from PubChem in order to compare them with the bioactive compounds from *A. indica* leaf.

2.2 Drug Likeness Prediction

Using the SwissADME tool (Daina *et al.*, 2017) (<http://www.swissadme.ch>) and the ADMETlab tool (Dong *et al.*, 2018), the ADMET (absorption, distribution, metabolism, excretion, and toxicity) and physicochemical properties of the identified secondary metabolites from neem leaf and the FDA COVID-19 approved drugs were predicted. Using the SwissADME online program (Daina *et al.*, 2017), these compounds' druggability or drug-likeness was predicted using Lipinski's rule of five. Using Lipinski's Rule (Lipinski *et al.*, 2001), which validates the property of an oral drug for the compounds, this online server assesses the compound's drug similarity. Solubility (LogP), topological polar surface area (TPSA), molecular weight (MW), number of hydrogen bond acceptors (No.HBA), number of hydrogen bond donors (No.HBD), and volume (Vol) are among the physicochemical parameters.

2.3 Bioactivity Prediction

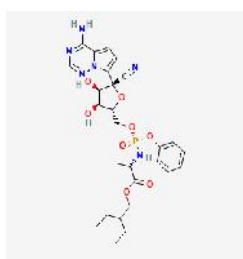
Using the Molinspiration server (www.molinspiration.com) (Diebold, 2003), the compounds were further examined for biological features (bioactivities). GPCR ligand, ion channel modulator, kinase inhibitor, nuclear receptor ligand, protease inhibitor, and enzyme inhibitor were among the six features predicted by molinspiration bioactivity.

3.0 Results

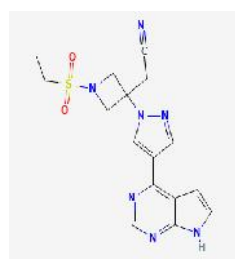
Table 1 showed the molecular formula and PubChem CID of the ligands investigated. Also, figure 1 showed the 2-D structures of the ligands as downloaded from PubChem.

Table 1: Ligands and Their PubChem CID

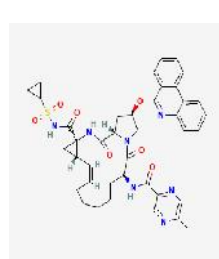
S/No	Ligands	PubChem CID	Molecular Formula
1.	Remdesivir	121304016	C ₂₇ H ₃₉ N ₆ O ₈ P
2.	Baricitinib	44205240	C ₁₆ H ₂₁ N ₇ O ₂ S
3.	Paritaprevir	45110509	C ₄₀ H ₄₃ N ₇ O ₇ S
4.	Ivermectin	6321424	C ₄₈ H ₇₄ O ₁₄
5.	2-monolinolenin	11674746	C ₂₁ H ₃₆ O ₄
6.	Azadirachtin A	4369359	C ₃₅ H ₄₄ O ₁₆
7.	Azadirachtin D	65981	C ₃₄ H ₄₄ O ₁₄₄
8.	Azadirachtin H	16134956	C ₃₃ H ₄₂ O ₁₄
9.	Azadirachtin F	131750885	C ₃₃ H ₄₄ O ₁₄
10.	Azadirachtin I	5281303	C ₃₂ H ₄₂ O ₁₂
11.	Desacetylnimbin	5281654	C ₂₈ H ₃₄ O ₈
12.	Azadiradione	5316860	C ₂₈ H ₃₄ O ₅
13.	Nimbin	108058	C ₃₀ H ₃₆ O ₉
14.	Nimbolin	6443005	C ₃₉ H ₄₆ O ₁₀
15.	Nimbolide	12313376	C ₂₇ H ₃₀ O ₇
16.	Nimbinene	44715635	C ₂₈ H ₃₄ O ₇
17.	Azadirone	10906239	C ₂₈ H ₃₆ O ₄



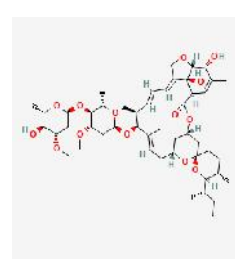
Remdesivir



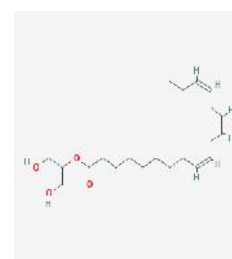
Baricitinib



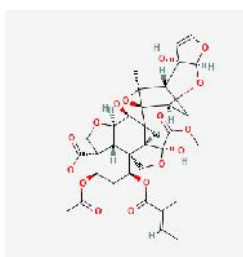
Paritaprevir



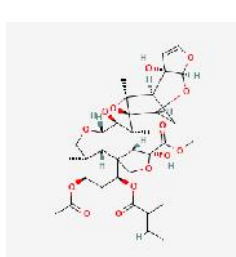
Ivermectin



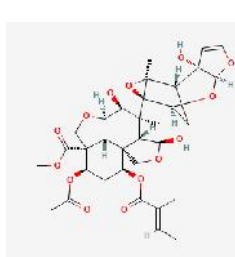
2-monolinolenin



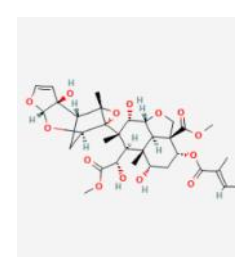
Azadirachtin A



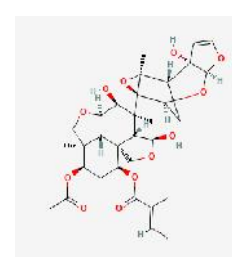
Azadirachtin D



Azadirachtin H



Azadirachtin F



Azadirachtin I

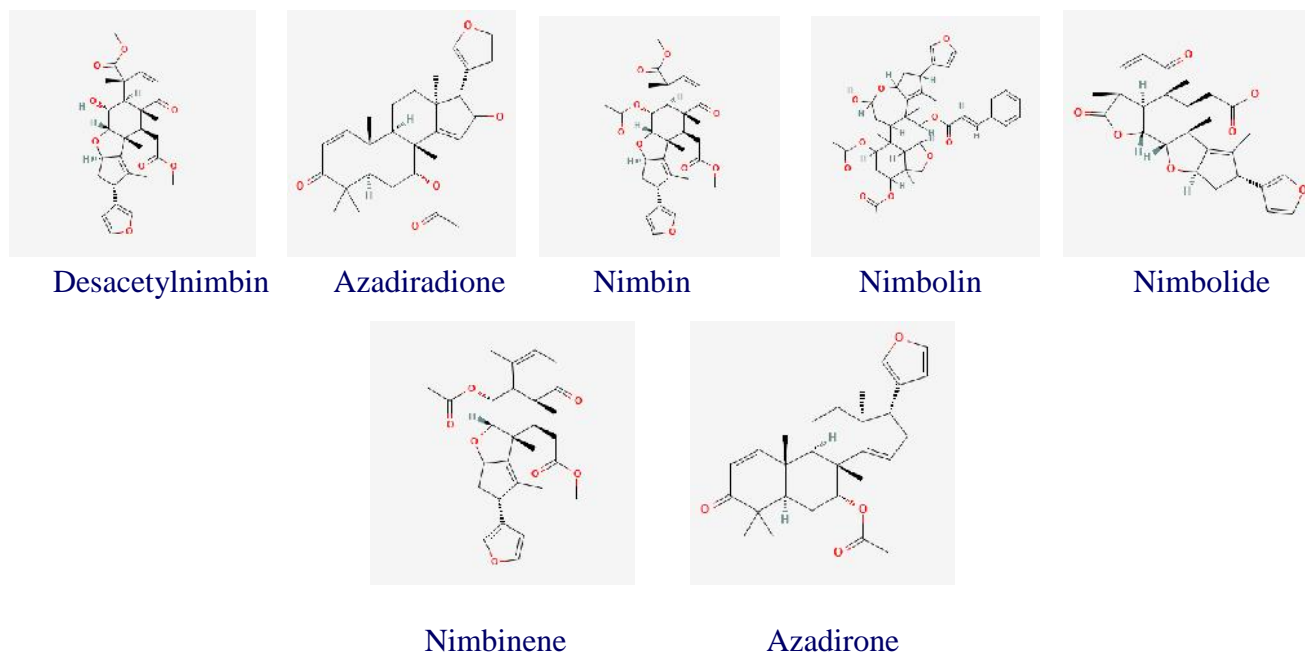


Figure 1: The 2-D Chemical Structures of the Ligands

Table 2: The Water Solubility of the Molecules

Properties Ligands	ESOL S (mg/ml)	ESOL Class	Ali S (mg/ml)	Ali Class	Silicos IT S (mg/ml)	Silicos IT Class
Remdesivir ²	0.184	Soluble	0.004	M Soluble	0.0115	M Soluble
Baricitinib ¹	7.31	V Soluble	10.60	V Soluble	0.0174	M Soluble
Paritaprevir ⁴	0.000049	P Soluble	0.0000022	P Soluble	0.00000014	P Soluble
Ivermectin ⁴	0.0000016	P Soluble	0.00000017	P Soluble	0.113	Soluble
2-monolinolenin ²	0.0316	M Soluble	0.000261	M Soluble	0.0404	Soluble
Azadirachtin A ²	0.0333	M Soluble	0.0045	M Soluble	28.60	V Soluble
Azadirachtin D ²	0.0106	M Soluble	0.00148	M Soluble	11.3	V Soluble
Azadirachtin H ²	0.034	M Soluble	0.00738	M Soluble	42.70	V Soluble
Azadirachtin F ²	0.0319	M Soluble	0.00319	M Soluble	68.30	V Soluble
Azadirachtin I ²	0.0107	M Soluble	0.00242	M Soluble	16.90	V Soluble
Desacetylnimbin ²	0.0961	M Soluble	0.0103	M Soluble	0.076	V Soluble
Azadiradione ⁴	0.00117	M Soluble	0.000359	P Soluble	0.000223	P Soluble
Nimbin ³	0.0345	M Soluble	0.0214	M Soluble	0.0019	M Soluble
Nimbolin ⁴	0.000182	P Soluble	0.0000431	P Soluble	0.0000745	P Soluble
Nimbolide ³	0.0530	M Soluble	0.0857	M Soluble	0.00249	M Soluble
Nimbinene ³	0.0719	M Soluble	0.1210	Soluble	0.00219	M Soluble
Azadirone ⁴	0.000373	P Soluble	0.0000926	P Soluble	0.000162	P Soluble

KEY: M= moderately; P= poorly; S= solubility

Table 2 above showed the results of the solubility of the ligands using different models. The qualitative estimation of the solubility class is given according to the following log *S* scale: insoluble <-10 <poorly <-6 <moderately <-4 <soluble <-2 <very <0 <highly. All the predicted

values in SwissADME are the decimal logarithm of the molar solubility in water (log *S*). Here, the ligands with superscripts 1, 2, 3 and 4 is said to be very soluble, soluble, moderately soluble and poorly soluble respectively.

Table 3: The Physicochemical Properties of the Ligands

Properties Ligands	MW(g/mol)	No HA	No Ar HA	F Csp3	No RB	No HBA	No HBD	MR	TPSA
Remdesivir	606.61	42	15	0.52	15	12	5	153.39	215.59
Baricitinib	375.45	26	14	0.44	6	7	2	101.47	131.17
Paritaprevir	765.88	55	20	0.42	9	10	3	211.96	198.03
Ivermectin	875.09	62	0	0.81	8	14	3	230.77	170.06
2-monolinolenin	352.51	25	0	0.67	17	4	2	105.25	66.76
Azadirachtin A	720.71	51	0	0.77	10	16	3	165.92	215.34
Azadirachtin D	676.7	48	0	0.79	8	14	3	159.83	189.04
Azadirachtin H	662.68	47	0	0.79	8	14	3	154.98	189.04
Azadirachtin F	664.69	47	0	0.79	9	14	4	157.18	200.04
Azadirachtin I	618.67	44	0	0.81	6	12	3	148.89	162.74
Desacetylnimbin	498.56	36	5	0.61	6	8	1	129.07	112.27
Azadiradione	450.57	33	5	0.61	3	5	0	125.48	73.58
Nimbin	540.6	39	5	0.60	8	9	0	138.81	118.34
Nimbolin	674.78	49	11	0.56	9	10	1	178.44	130.73
Nimbolide	466.52	34	5	0.59	4	7	0	120.00	92.04
Nimbinene	482.57	35	5	0.61	6	7	0	128.17	92.04
Azadirone	436.58	32	5	0.64	3	4	0	125.28	56.51

KEY: MW= Molecular weight; No HA= Number of heavy atoms; No Ar HA= Number of aromatic heavy atoms; F= fraction; No RB= Number of rotatable bonds; No HBA= Number of hydrogen bond acceptors; No of HBD= Number of hydrogen bond donors; MR= molecular refractivity; TPSA= Topological polar surface area.

Table 4: The Lipophilicity of the Ligands

Models Ligands	ILOGP	XLOGP3	WLOGP	MLOGP	SILICOS-IT	Consensus Log $P_{o/w}$
Remdesivir	3.71	1.02	1.65	0.26	-0.41	1.24
Baricitinib	1.81	-0.73	1.23	-0.51	0.24	0.41
Paritaprevir	2.03	4.65	3.89	0.88	2.28	2.75
Ivermectin	5.93	6.34	5.60	1.25	2.72	4.37
2-monolinolenin	4.73	4.99	4.47	3.33	5.76	4.66
Azadirachtin A	3.90	1.09	-0.20	-0.47	1.07	1.08
Azadirachtin D	3.40	2.06	0.64	0.09	1.54	1.55
Azadirachtin H	3.09	1.38	0.25	-0.09	1.02	1.13
Azadirachtin F	2.84	1.51	-0.11	-0.50	1.14	0.98
Azadirachtin I	3.63	2.35	1.10	0.49	1.15	1.81
Desacetylnimbin	3.61	1.71	3.35	1.69	3.43	2.76
Azadiradione	3.17	4.82	5.42	3.28	5.00	4.34
Nimbin	3.98	2.28	3.92	2.04	3.96	3.24
Nimbolin	3.84	4.72	5.64	3.16	4.96	4.46
Nimbolide	3.51	2.17	3.74	2.28	3.83	3.11
Nimbinene	3.83	2.04	4.52	2.48	4.32	3.44
Azadirone	3.86	5.72	6.24	4.19	5.30	5.06

According to Lipinski's Rule of 5, an oral drug should have a LogP value <5, of which all our compounds were within the limit. For good oral and intestinal absorption of a compound,

lipophilicity should ideally fall between 1.35-1.8. Thus from this result, all the ligands have LogP values less than 5 with exception of azadirone.

Table 5: The Druglikeness and Medicinal Chemistry of the Molecules

Parameters Ligands	Lip V	GV	Veber V	EV	MV	B Score	PAINS Alert	Brenk Alert	LL	SA
Remdesivir	2	3	3	1	3	0.17	0	1	2	6.59
Baricitinib	0	0	0	0	0	0.55	0	0	1	3.21
Paritaprevir	2	3	1	1	3	0.17	0	2	3	6.97
Ivermectin	2	4	1	1	4	0.17	0	1	3	10.00
2-monolinolenin	0	0	1	0	1	0.55	0	1	3	3.65
Azadirachtin A	2	3	1	1	4	0.17	0	3	3	8.11
Azadirachtin D	2	3	1	1	4	0.17	0	3	2	7.96
Azadirachtin H	2	3	1	1	4	0.17	0	3	2	7.87
Azadirachtin F	2	3	1	1	3	0.17	0	3	2	7.50
Azadirachtin I	2	3	1	1	4	0.17	0	3	1	7.74
Desacetylnimbin	0	1	0	0	0	0.55	0	2	1	6.32
Azadiradione	0	0	0	0	0	0.55	0	0	2	5.89
Nimbin	1	3	0	0	0	0.55	0	2	2	6.54
Nimbolin	1	4	0	0	1	0.55	0	3	3	7.47
Nimbolide	0	0	0	0	0	0.55	0	2	1	6.07
Nimbinene	0	1	0	0	0	0.55	0	2	1	6.21
Azadirone	1	1	0	1	1	0.55	0	1	2	5.87

Key: Lip V= Lipinski Violation; B= Bioavailability; LL= lead likeness; GV= Ghose Violation; MV = Muegge Violation; EV = Egen Violation; SA= Synthetic accessibility.

The numbers, 0, 1, 2, 3 and 4 were categorical values which respectively indicates no (zero), one, two, three and four violations of the rules. Any ligands that do not have more than one violation could be said to have a good drug-

likeness and possibly lead-likeness. From this result, baricitinib, 2-monolinolenin, desacetylnimbin, azadiradione, nimbin, nimbolin, nimbolide, nimbinene and azadirone have one or no violation.

Table 6: The Metabolism and Distribution of the Ligands

Properties Molecules	GIA	BBB P	P-gp S	C1A2I	C2C19I	C2C9I	C2D6I	C3A4I	Log K _p (cm/s)
Remdesivir	Low	No	Yes	No	No	No	No	Yes	-9.28
Baricitinib	High	No	Yes	No	No	No	No	No	-9.11
Paritaprevir	Low	No	Yes	No	No	No	No	Yes	-7.67
Ivermectin	Low	No	Yes	No	No	No	No	No	-7.14
2-monolinolenin	High	Yes	No	No	No	No	Yes	Yes	-4.91
Azadirachtin A	Low	No	Yes	No	No	No	No	No	-9.92
Azadirachtin D	Low	No	Yes	No	No	No	No	No	-8.97
Azadirachtin H	Low	No	Yes	No	No	No	No	No	-9.36
Azadirachtin F	Low	No	Yes	No	No	No	No	No	-9.28
Azadirachtin I	Low	No	Yes	No	No	No	No	No	-8.41
Desacetylnimbin	High	No	No	No	No	No	No	Yes	-8.13
Azadiradione	High	No	Yes	No	No	No	No	No	-5.63
Nimbin	High	No	No	No	No	No	No	No	-7.98
Nimbolin	Low	No	Yes	No	No	No	No	No	-7.06
Nimbolide	High	No	Yes	No	No	No	No	No	-7.61
Nimbinene	High	No	No	No	No	No	Yes	Yes	-7.8
Azadirone	High	No	No	No	No	Yes	No	No	-4.9

KEY: GIA= gastrointestinal absorption; P= permeant; P-gp= P-glycoprotein; S=substrate, I= inhibitor; C=CYP (cytochrome P-450); Log K_p= skin permeation.

Yes and No respectively connote higher probability of the ligand to be substrate and non-substrate of P-gp and inhibitor and non-inhibitor of given P450 isoforms.

Table 7: Excretion and Toxicity of the Ligand

Parameters Ligands	Excretion		Toxicity					
	T ^{1/2} (Hr) (mL/min/kg)	CL	hERG Blocker	H-HT	AMES	SkinSen	LD ₅₀ (log[1/mol/kg])	DILI
Remdesivir	1.39	0.74	1	1	0	0	2.99	1
Baricitinib	1.47	1.16	0	1	0	0	2.52	1
Paritaprevir	2.19	0.82	1	0	0	0	3.10	1
Ivermectin	2.43	1.04	1	0	0	0	3.68	0
2-monolinolenin	1.80	1.60	1	0	0	1	1.46	0
Azadirachtin A	2.05	1.37	0	0	0	0	3.74	0
Azadirachtin D	1.94	1.38	0	0	0	0	3.73	0
Azadirachtin H	1.92	1.49	0	0	0	0	3.86	0
Azadirachtin F	1.99	1.53	0	0	0	0	3.94	0
Azadirachtin I	1.75	1.46	0	0	0	0	3.98	0
Desacetylnimbin	1.45	1.77	0	0	0	0	3.76	0
Azadiradione	1.73	1.88	0	1	0	0	3.59	0
Nimbin	1.69	1.65	0	1	0	0	3.76	1
Nimbolin	2.15	1.60	1	1	0	0	4.25	1
Nimbolide	1.41	1.92	0	0	0	0	3.94	1
Nimbinene	1.41	1.77	0	1	0	0	3.70	0
Azadirone	1.87	1.70	1	1	0	0	3.42	0

Keys; T^{1/2} =Half-time; CL= clearance; hERG=human ether-a-go-go-related gene; H-HT= human hepatotoxicity; AMES= Ames mutagenicity; SkinSen= skin sensitivity; LD₅₀= median lethal dose; DILI=drug induced liver injury.

Note that 1 and 0 are categorical which mean **positive** and **negative** respectively with different probabilities (although not shown here). For

instance, hERG 0 means non-blocker while 1 means blocker.

Table 8: Bioactivity Prediction of the Ligands using Molinspiration Software

Bioactivity Ligands	Bioactivity Scores					
	GPCR L	ICM	Kinase I	NRL	Protease I	Enzyme I
Remdesivir	0.35	-0.27	0.26	-0.46	0.54	0.44
Baricitinib	0.52	0.12	0.80	-0.69	0.15	0.28
Paritaprevir	-0.78	-2.24	-1.79	-2.15	0.22	-1.24
Ivermectin	-2.49	-2.86	-3.23	-2.94	-1.89	-2.53
2-monolinolenin	0.38	0.13	0.02	0.26	0.20	0.43
Azadirachtin A	-0.71	-1.51	-1.46	-0.67	-0.35	-0.71
Azadirachtin D	-0.36	-1.00	-1.02	-0.16	-0.10	-0.28
Azadirachtin H	-0.17	-0.81	-0.89	-0.03	0.13	-0.12
Azadirachtin F	-0.20	-0.79	-0.94	-0.06	0.03	-0.08
Azadirachtin I	0.07	-0.42	-0.57	0.34	0.29	0.21
Desacetylnimbin	0.31	0.21	-0.22	0.35	0.16	0.43
Azadiradione	0.08	0.07	-0.51	0.44	-0.01	0.41
Nimbin	0.24	0.14	-0.30	0.26	0.10	0.36
Nimbolin	-0.45	-1.11	-1.12	-0.59	-0.23	-0.47
Nimbolide	0.22	0.20	-0.36	0.32	0.04	0.36
Nimbinene	0.21	0.18	-0.30	0.37	0.04	0.33
Azadirone	0.13	0.11	-0.54	0.47	0.06	0.44

Keys: GPCRL= G-protein coupled receptor ligand; ICM= Ion channel modulator; I= inhibitor; NRL= Nuclear receptor ligand

The blue coloured values signify the ligands with significant bioactivity as predicted by Molinspiration Software, which increases as the value increases.

4.0 Discussion and Conclusion

4.1 Discussions

When compared to FDA-approved COVID-19 medications in this study, the results of this in-silico ADMET and bioactivity prediction of important secondary metabolites from *A. indica* leaf from Loganathan et al. (2021) revealed noteworthy results. Two (40%) of the five FDA COVID-19 medications and three (25%) of the twelve secondary metabolites from *A. indica* leaf were deemed to be poorly soluble according to the solubility prediction (Table 2). Similar to what was found in this work, the physicochemical

characteristics of the ligands (Table 3) predict that the fraction of carbon Sp3 will fall between 0.25 and 1. For the purpose of determining the unsaturation and flexibility of the chosen ligands or compounds, the number of rotatable bonds should not be greater than 9. Furthermore, molecules with TPSAs greater than 140 angstroms squared (2) have a propensity to have poor cell membrane penetration. A TPSA of less than 90 is often required for molecules to pass through the BBB and act on receptors in the central nervous system, as illustrated in the case of the 2-monolinolenin molecule (Fig. 3). The likelihood that an oral medication candidate would be developed successfully and the number of aromatic rings are not inversely related. Oral medication candidates with more than three aromatic rings are less likely to be developed successfully than those with fewer.

For a large number of compounds, it might be challenging to experimentally determine the lipophilicity (LogP), which is the ability of a molecule to differentially dissolve in a mixture of water and lipids or organic solvents. P is therefore designed to help prioritize the synthesis of the right chemicals and reduce the risks and failures associated with innovative drug candidates. In fact, LogP is a crucial element of Lipinski's Rule of Five recommendations, which predict a novel synthetic compound's drug-likeness. Lipinski's Rule of 5, which stipulates that an oral drug should have a LogP value of less than 5, was met by all of our compounds. An optimal range for lipophilicity for a compound's oral and intestinal absorption is 1.35–1.8. Thus from this result (Table 4), all the ligands have LogP values less than 5 with exception of azadirone.

The models supporting the predictors for lipophilicity should be as varied as feasible in order to increase the prediction precision by consensus log Po/w (Mannhold *et al.*, 2009). As a result, SwissADME provided access to five publicly available predictive models, including XLOGP3, an atomistic method with corrective factors and a knowledge-based library (Cheng *et al.*, 2007), WLOGP, an internal implementation of a purely atomistic method based on the fragmental system of Wildman and Crippen (Wildman and Crippen, 1999), and MLOGP, an exemplary topological method relying on a linear relationship with 13 mole. The LogP numbers are reasonably accurate because the consensus log P_{o/w} is the arithmetic mean of the values anticipated by the five suggested approaches.

The druggability or drug-likeness of ligands was determined through structural or physicochemical examinations of development compounds that were sufficiently advanced to be recognized as oral drug candidates. It is common practice to utilize this method to screen chemical libraries for compounds with properties that are most likely incompatible with a desired pharmacokinetic profile. In this study, the Swiss ADME Model gave researchers access to five different rule-based filters, each of which has a distinct set of characteristics that distinguish a molecule as

being drug-like. These filters usually come about as a result of research projects carried out by large pharmaceutical companies to raise the standard of their in-house chemical collections. The Lipinski (Pfizer) filter was used to implement the rule-of-five for the first time (Lipinski *et al.*, 2001). The Ghose (Amgen), Veber (GSK), Egan (Pharmacia), and Muegge (Bayer) methodologies were taken from, in that order, Ghose *et al.* (1999), Veber *et al.* (2002), Egan *et al.* (2000), and Muegge *et al.* (2001). Multiple estimates allow for group consensus or the selection of strategies most suited to the end-user's particular needs in terms of chemical space or project-related factors. The Abbot Bioavailability Score (Martin *et al.*, 2005) was also developed to predict whether a substance will have at least 10% oral bioavailability in rats or detectable Caco-2 permeability in rats. Based on total charge, TPSA, and Lipinski filter violation, this semi-quantitative rule-based score creates four classes of compounds with probabilities of 11%, 17%, 56%, or 85%. Baricitinib, 2-monolinolenin, desacetylnimbin, azadiradione, nimbin, nimbolin, nimbolide, nimbinene, and azadirone all have bioactivity scores in this study that are greater than 50%, which is consistent with their drug-likeness.

The detection of potentially problematic components is made possible by two complementary pattern recognition techniques, which aid medicinal (bio)chemists in their continual quest to find new medications. PAINS (pan-assay interference chemicals) are ligands or compounds with substructures that demonstrate a strong reaction in assays regardless of the protein target. They are also referred to as frequent hits or promiscuous compounds. Baell and Holloway (2010) found such components that lead to falsely positive biological output after looking at six orthogonal assays. Structural Alert, a list of 105 fragments that Brenk *et al.* (2008) found to be potentially dangerous, chemically reactive, metabolically unstable, or to have characteristics that lead to poor pharmacokinetics, is another feature of SwissADME tools. Because it is crucial for a (bio)chemist to decide whether a certain molecule is suited to start lead optimization,

SwissADME designed a rule-based technique for leadlikeness that was adapted from Teague *et al.* (1999). Based on this finding, only Brenk Alert has a PAIN Alert. In a manner similar to this, only 5 of the chemicals under investigation (Table 5) display less than 2 LL breaches. Another crucial aspect of computer-aided drug design (CADD) procedures is the capability to select the most promising virtual compounds that will be produced and analyzed in biological tests or other research. Another important element to take into account in lead optimization is synthetic accessibility (SA). The parameters used to describe size and complexity, such as macrocycles, chiral centers, or spiro functions as described by Ertl and Schuffenhauer in 2009, are added together for a specific molecule to calculate the fragmental contributions to SA. The SA Score, which has undergone standardization, goes from 1 (extremely easy) to 10 (very tough). So, the simpler the chemical can be produced, the lower the SA Score.

Potts and Guy (1992) found that the skin permeability coefficient (K_p) was linearly associated with molecule size and lipophilicity ($R^2 = 0.67$), which led to the development of the multiple linear regression method used to predict K_p . The molecule becomes less permeable to skin as $\log K_p$ (with K_p in cm/s) becomes more negative. As a result, the values in red on Table 6 had comparatively low skin sensitivity, whereas the values in blue had significant skin sensitivity. Knowing which substances are substrates or non-substrates of the permeability glycoprotein (P-gp, the most significant member among ATP-binding cassette transporters, or ABC-transporters) is also necessary for assessing active efflux through biological membranes, such as from the brain or from the gastrointestinal wall to the lumen (Montanari and Ecker 2015). P-gp has a number of important functions, one of which is the selective transportation of xenobiotics away from the central nervous system (CNS) (Szakács *et al.*, 2008). It is also critical to comprehend how substances interact with cytochromes P450 (CYP). This superfamily of isoenzymes contributes significantly to drug clearance through metabolic biotransformation (Testa and Kraemer

2007). In order to improve tissue and organism protection, van Waterschoot and Schinkel (2011) found that CYP and P-gp can metabolize tiny substances in a synergistic manner. Inhibition of these isoenzymes undoubtedly plays a significant role in pharmacokinetics-related drug-drug interactions (Huang *et al.*, 2008; Hollenberg, 2011), which can have toxic or other unfavorable side effects (Kirchmair *et al.*, 2015). This is due to the lower clearance and accumulation of drugs or their metabolites. Numerous CYP isoform inhibitors have been found. While some have an effect on several CYP isoforms, others show selectivity for certain isoenzymes (Veith *et al.*, 2009). Therefore, it is essential to predict a molecule's propensity to inhibit CYPs and cause major drug interactions as well as identify which isoforms are affected during the drug development process. Only remdesivir, paritaprevir, 2-monolinolenin, desacetylnimbin, and nimbinene inhibited one or more isoforms, as stated in Table 6 above. The FDA has approved 2-monolinolenin for the treatment of COVID-19, but it is the only medicine that can cross the blood-brain barrier (BBB; Table 6).

With the exception of remdesivir and nimbolin, the majority of the medicines exhibited low toxicity according to the toxicity prediction (Table 7). Similar to this, all the compounds, with the exception of 2-monolinolenin, showed little oral acute toxicity (Lei *et al.*, 2016). With the exception of remdesivir and paritaprevir, all of the medications have an excretion half-life of 1 to slightly less than 3 hours and a clearance time of around 2 mL/min/kg (Table 7). In the study of bioactivity prediction, the ligands with significant bioactivity as predicted by Molinspiration Software are represented by blue-colored values; the value rises as the value rises (Table 8). This discovery indicates that nimbolin, ivermectin, azadirachtin A, azadirachtin D, azadirachtin H, and azadirachtin F did not display any bioactivity. This was not unexpected given the comparatively subpar ADMET characteristics of these ligands. Many of the ligands under investigation may also function as inhibitors of enzymes and nuclear receptor ligands. Only two substances, remdesivir

and baricitinib, might, however, inhibit kinases (Table 8).

Significance of the Study: This work has shown that many distinct bioactive substances found in *A. indica* leaves, when isolated and investigated (via molecular docking, in-vitro, and in-vivo experiments), could result in the discovery of drug(s) for treating COVID-19. Examples of these compounds are azadiradione and nimbolide.

4. 2 Conclusion

The majority of the *A. indica* bioactive secondary metabolites exhibited favorable ADMET and bioactivity characteristics. Ivermectin, azadirachtin A, azadirachtin D, azadirachtin H, azadirachtin F, azadirachtin I, and nimbolin, on the other hand, have shown comparatively subpar properties. Additionally, the *A. indica* compounds outperformed the FDA-approved COVID-19 medication in terms of their characteristics. Similar to this, all of the substances except for remdesivir and nimbolin have a relatively low level of toxicity. With the exception of 2-monolinolenin, their oral acute toxicity can be deemed to be rather modest.


References

- Baell, J. B. and Holloway, G. A. (2010). New substructure filters for removal of pan assay interference compounds (PAINS) from screening libraries and for their exclusion in bioassays. *J. Med. Chem.*; 53: 2719–2740.
- Biswas, K., Chattopadhyay, I., Banerjee, R.K. and Bandyopadhyay, U. (2002). Biological activities and medicinal properties of neem (*Azadirachta indica*). *Current Science*; 13:36-45.
- Borkotoky, S. and Banerjee, M. (2020). A computational prediction of SARS-CoV-2 structural protein inhibitors from *Azadirachta indica* (Neem). *Journal of Biomolecular Structure and Dynamics*; 8:1-1. <https://doi.org/10.1080/07391102.2020.1774419>
- Brenk, R., Schipani, A., James, D., Krasowski, A., Gilbert, L., Frearson, J and Wyatt, P.G (2008). Lessons learnt from assembling screening libraries for drug discovery for neglected diseases. *Chem. Med. Chem.*; 3: 435–444. doi: [10.1002/cmdc.200700139](https://doi.org/10.1002/cmdc.200700139)
- Britto, A.J. and Sheeba, D.H. (2011). *Azadirachta indica* juss – a potential antimicrobial agent, *International Journal of Applied Biological and Pharmaceutical Technology*; 4550–4557.
- Cheng, T., Zhao, Y., Li, X., Lin, F., Xu, Y., Zhang, X., Li, Y., Wang, R. and Lai L. (2007). Computation of Octanol–Water Partition Coefficients by Guiding an Additive Model with Knowledge. *J. Chem. Inf. Model*; 47(6): 2140–2148. doi: 10.1021/ci700257y.
- Daina, A., Olivier, M. and Vincent, Z. (2017). SwissADME: a free web tool to evaluate pharmacokinetics, drug-likeness and medicinal chemistry friendliness of small molecules. *Scientific Report*; 7:42717. DOI: [10.1038/srep42717](https://doi.org/10.1038/srep42717)
- Diebold, U. (2003). The surface science of titanium dioxide. *Surf. Sci. Rep.*; 48: 53–229, [https://doi.org/10.1016/S0167-5729\(02\)00100-0](https://doi.org/10.1016/S0167-5729(02)00100-0).
- Dong, J., Wang, N., Yao, Z., Zhang, L., Cheng, Y., Ouyang, D., Lu, L. and Cao, D. (2018). ADMETlab: a platform for systematic ADMET evaluation based on a comprehensively collected ADMET database. *Journal of Cheminformatics*; 10:29.
- Egan, W. J., Merz, K. M. and Baldwin, J. J. (2000). Prediction of Drug Absorption Using Multivariate Statistics. *J. Med. Chem.*; 43: 3867–3877.
- El-Hawary, S.S., El-Tantawy, M.E., Rabeh, M.A. and Badr, W.K. (2013). Chemical composition and biological activities of essential oils of *Azadirachta indica* A. Juss. *International Journal of Applied Research in Natural Products*; 6: 33-42.
- Ertl, P. and Schuffenhauer, A. (2009). Estimation of synthetic accessibility score of drug-like molecules based on molecular

- complexity and fragment contributions. *J. Cheminform*; 1: 8.
- Fernandes, S.R., Barreiros, L., Oliveira, R.F., Cruz, A., Prudêncio, C., Oliveira, A.I., Pinho, C., Santos, N. and Morgado, J. (2019). Chemistry, bioactivities, extraction and analysis of azadirachtin: State-of-the-art. *Fitoterapia*; 134:141-150. <https://doi.org/10.1016/j.fitote.2019.02.006>
- Ghimeray, A.K., Jin, C.W., Ghimire, B.K. and Che, D.H. (2009). Antioxidant activity and quantitative estimation of *Azadirachtin* and Nimbin in *Azadirachta indica*; *African Journal of Biotechnology*; 54: 1684–5315.
- Ghose, A. K., Viswanadhan, V. N. and Wendoloski, J. J. (1999). A knowledge-based approach in designing combinatorial or medicinal chemistry libraries for drug discovery. A qualitative and quantitative characterization of known drug databases. *J. Comb. Chem.*;1: 55–68.
- Hoffmann, M., Kleine-Weber, H., Schroeder, S., Krüger, N., Herrler, T., Erichsen, S., et al. (2020). “SARS-CoV-2 Cell Entry Depends on ACE2 and TMPRSS2 and Is Blocked by a Clinically Proven Protease Inhibitor”. *Cell*. 181(2): 271–280. [doi:10.1016/j.cell.2020.02.052](https://doi.org/10.1016/j.cell.2020.02.052). [PMC 7102627](https://pubmed.ncbi.nlm.nih.gov/32142651/). [PMID 32142651](https://pubmed.ncbi.nlm.nih.gov/32142651/).
- Hollenberg, P. F. (2002). Characteristics and common properties of inhibitors, inducers, and activators of CYP enzymes. *Drug Metab. Rev.*; 34: 17–35.
- Hossain, M.A. and Nagooru, M.R. (2011). Biochemical profiling and total flavonoids contents of leaves crude extract of endemic medicinal plant, *Corydiline terminalis* L. Kunth. *Pharmacognosy Journal*; 3: 25–30.
- Hossaina, M.A., Al-Toubia, W. A.S., Welia, A.M., Al-Riyamia, Q.A. and Al-Sabahib, J.N. (2013). Identification and characterization of chemical compounds in different crude extracts from leaves of Omani. *Journal of Taibah University for Science*; 7: 181-188.
- Hu, B., Guo, H., Zhou, P. and Shi, Z. (2021). Characteristics of SARS-CoV-2 and COVID-19: Review. *Nature Microbiology*; 19:141-154.
- Huang, S.M., Strong, J.M., Zhang, L., Reynolds, K.S., Nallani, S., Temple, R., Abraham, S., Habet, S.A., Baweja, R.K., Burckart, G.J., Chung, S., Colangelo, P., Frucht, D., Green, M.D., Hepp, P., Karnaukhova, E., Ko, H.S., Lee, J.I., Marroum, P.J., Norden, J.M., Qiu, W., Rahman, A., Sobel, S., Stifano, T., Thummel, K., Wei, X.X., Yasuda, S., Zheng, J.H., Zhao, H. and Lesko, L.J. (2008). New era in drug interaction evaluation: US Food and Drug Administration update on CYP enzymes, transporters, and the guidance process. *J. Clin. Pharmacol.*; 48: 662–670. [doi:10.1177/0091270007312153](https://doi.org/10.1177/0091270007312153).
- International Committee on Taxonomy of Viruses for Coronaviridae Study Group. (2020). The species severe acute respiratory syndrome- related coronavirus: classifying 2019-nCoV and naming it SARS- CoV-2. *Nat. Microbiol.* 5: 536–544.
- Kim, S., Thiessen, P. A., Bolton, E. E., Chen, J., Fu, G., Gindulyte, A., Han, L., He, J., He, S., Shoemaker, B. A., Wang, J., Yu, B., Zhang, J., and Bryant, S. H. (2016). PubChem Substance and Compound databases. *Nucleic acids research*; 44(D1): D1202–D1213.
- Kirchmair, J., Göller, A.H., Lang, D., Kunze, J., Testa, B., Wilson, I.D., Glen, R.C. and Schneider, G. (2015). Predicting drug metabolism: experiment and/or computation? *Nature Rev. Drug Discov.*; 14: 387–404. [doi: 10.1038/nrd4581](https://doi.org/10.1038/nrd4581).
- Lei, T., Li, Y., Song, Y., Li, D., Sun, H. and Hou, T. (2016). ADMET evaluation in drug discovery: Accurate prediction of rat oral acute toxicity using relevance vector machine and consensus modeling. *Journal of Cheminformatics*; 8(6): 1-19.
- Lipinski, C.A., Lombardo, F., Dominy, B.W. and Feeney, P.J. (2001). Experimental and computational approaches to estimate solubility and permeability in drug discovery and development settings. *Adv. Drug Deliv. Rev.*; 46: 3-26,

- [https://doi.org/10.1016/s0169-409x\(00\)00129-0](https://doi.org/10.1016/s0169-409x(00)00129-0).
- Loganathan, T., Barathinivas, A., Soorya, C., Balamurugan, S., Nagajothi, T.G., Ramya, S. and Jayakumararaj, R. (2021). GCMS Profile of Bioactive Secondary Metabolites with Therapeutic Potential in the Ethanolic Leaf Extracts of *Azadirachta indica*: A Sacred Traditional Medicinal Plant of INDIA. *Journal of Drug Delivery and Therapeutics*; 11(4-S):119-126 DOI: <http://dx.doi.org/10.22270/jddt.v11i4-S.4967>.
- Mannhold, R., Poda, G. I. and Ostermann, C. (2009). Calculation of molecular lipophilicity: State of the art and comparison of logP methods on more than 96,000 compounds. *J. Pharm. Sci.*; 98: 861–893.
- Martin, S., Roe, D. and Faulon, J.L. (2005). Predicting protein-protein interactions using signature products. *Bioinformatics* 21(2):218-26. <https://doi.org/10.1093/bioinformatics/bth483>
- Muegge, I., Heald, S.L. and Brittelli, D. (2001). Simple selection criteria for drug-like chemical matter. *J Med Chem.*; 44(12):1841-6. doi: [10.1021/jm015507e](https://doi.org/10.1021/jm015507e).
- Mehta, P., McAuley, D.F., Brown, M., Sanchez, E., Tattersall, R.S. and Manson, J.J. (2020). COVID-19: consider cytokine storm syndromes and immune-suppression. *Lancet*; 395: 1033-1034. doi: [10.1016/S0140-6736\(20\)30628-0](https://doi.org/10.1016/S0140-6736(20)30628-0).
- Mohammad, M. S. and Forough, M. (2007). Investigation of Compounds from *Azadirachta indica* (Neem). *Asian Journal of Plant Sciences*; 6: 444-445. DOI: [10.3923/ajps.2007.444.445](https://doi.org/10.3923/ajps.2007.444.445)
- Montanari, F. and Ecker, G. F. (2015). Prediction of drug-ABC-transporter interaction–Recent advances and future challenges. *Adv. Drug Deliv. Rev.*; 86: 17–26.
- Monteil, V., Kwon, H., Prado, P., Hagelkrüys, A., Wimmer, R.A., Stahl, M., Leopoldi, A., Garreta, E., Hurtado Del Pozo, C., Prosper, F., Romero, J.P., Wirnsberger, G., Zhang, H., Slutsky, A.S., Conder, R., Montserrat, N., Mirazimi, A. and Penninger, J.M. (2020). Inhibition of SARS- CoV-2 infections in engineered human tissues using clinical- grade soluble human ACE2. *Cell*; 181(4): 905–913. doi: [10.1016/j.cell.2020.04.004](https://doi.org/10.1016/j.cell.2020.04.004).
- Moriguchi, I., Shuichi, H., Nakagome, I. and Hirano, H. (1994). Comparison of reliability of logP values for Drugs calculated by several methods. *Chem. Pharm. Bull.*; 42: 976–978.
- Muhammed, D., Odey, B.O., Alozieuwa, B.U., Alawode, R.A., Okunlola, B.M., Ibrahim, J., Lawal, A. and Berinyuy, E.B. (2021). Azadirachtin-A a bioactive compound from *Azadirachta indica* is a potential inhibitor of SARS-CoV-2 main protease. *AROC in Pharmaceutical and Biotechnology*; 1(1):1-8.
- Pandey, I.P., Ahmed, S.F., Chhimwal, S. and Pandey, S. (2012). Chemical composition and wound healing activity of volatile oil of leaves of *Azadirachta indica* A. juss. *Advances in Pure and Applied Chemistry*; 62: 2167-0854.
- Prashanth G.K. and Krishnaiah, G.M. (2014). Chemical composition of the leaves of *Azadirachta Indica* Linn (Neem). *International Journal of Advancement in Engineering Technology, Management and Applied Science*; 1(5): 21-31.
- Potts, R.O. and Guy, R.H. (1992). Predicting skin permeability. *Pharm Res.*; 9(5):663-669. doi: [10.1023/a:1015810312465](https://doi.org/10.1023/a:1015810312465).
- Szakács, G., Váradi, A., Ozvegy-Laczka, C. and Sarkadi, B. (2008). The role of ABC transporters in drug absorption, distribution, metabolism, excretion and toxicity (ADME-Tox). *Drug Discov. Today*; 13: 379–393.
- Teague, S.J., Davis, A.M., Leeson, P.D., Oprea, T. (1999). The Design of Leadlike Combinatorial Libraries. *Angew Chem Int Ed Engl.*; 38(24):3743-3748. doi: [10.1002/\(SICI\)1521-3773\(19991216\)38](https://doi.org/10.1002/(SICI)1521-3773(19991216)38).
- Testa, B. and Kraemer, S. D. (2007). *The Biochemistry of Drug Metabolism – An Introduction - Testa - 2007 - Chemistry*

- and Biodiversity - Wiley Online Library. *Chem. Biodivers.*
- Tian, X., Li, C., Huang, A., Xia, S., Lu, S., Shi, Z., Lu, L., Jiang, S., Yang, Z., Wu, Y. and Ying, T. (2020). Potent binding of 2019 novel coronavirus spike protein by a SARS coronavirus specific human monoclonal antibody. *Emerg. Microbes Infect.*; 9: 382–385. doi: [10.1080/22221751.2020.1729069](https://doi.org/10.1080/22221751.2020.1729069).
- van Waterschoot, R. A. B. and Schinkel, A. H. (2011). A critical analysis of the interplay between cytochrome P450 3A and P-glycoprotein: recent insights from knockout and transgenic mice. *Pharmacological Reviews*; 63: 390–410.
- Veber, D. F., Johnson, S.R., Cheng, H.Y., Smith, B.R., Ward, K.W. and Kopple, K.D. (2002). Molecular properties that influence the oral bioavailability of drug candidates. *J. Med. Chem.*; 45: 2615–2623. doi: [10.1021/jm020017n](https://doi.org/10.1021/jm020017n).
- Veith, H., Southall. N., Huang, R., James, T., Fayne, D., Artemenko, N., Shen, M., Inglese, J., Austin, C.P., Lloyd, D.G. and Auld, D.S. (2009). Comprehensive characterization of cytochrome P450 isozyme selectivity across chemical libraries. *Nature Biotechnol.*; 27(11): 1050–1055. doi: [10.1038/nbt.1581](https://doi.org/10.1038/nbt.1581).
- Wildman, S. A. and Crippen, G. M. (1999). Prediction of Physicochemical Parameters by Atomic Contributions. *J. Chem. Inf. Model.*; 39: 868–873.
- Xia, S., Liu, M., Wang, C., Xu, W., Lan, Q., Feng, S., Qi, F., Bao, L., Du, L., Liu, S., Qin, C., Sun, F., Shi, Z., Zhu, Y., Jiang, S. and Lu L. (2020). Inhibition of SARS-CoV-2 (previously 2019-nCoV) infection by a highly potent pan-coronavirus fusion inhibitor targeting its spike protein that harbors a high capacity to mediate membrane fusion. *Cell Res.*; 30(4): 343–355. doi: [10.1038/s41422-020-0305-x](https://doi.org/10.1038/s41422-020-0305-x).
- Zhou, P., Yang, X.L., Wang, X.G., Hu, B., Zhang, L., Zhang, W., Si, H.R., Zhu, Y., Li, B., Huang, C.L., Chen, H.D., Chen, J., Luo, Y., Guo, H., Jiang, R.D., Liu, M.Q., Chen, Y., Shen, X.R., Wang, X., Zheng, X.S., Zhao, K., Chen, Q.J., Deng, F., Liu, L.L., Yan, B., Zhan, F.X., Wang, Y.Y., Xiao, G.F. and Shi, Z.L. (2020). A pneumonia outbreak associated with a new coronavirus of probable bat origin. *Nature*; 579(7798): 270–273. doi: [10.1038/s41586-020-2012-7](https://doi.org/10.1038/s41586-020-2012-7).

Access this Article in Online	
	Website: www.ijarbs.com
	Subject: Cheminformatics
Quick Response Code	
DOI: 10.22192/ijarbs.2023.10.09.010	

How to cite this article:

Paul Chijioke OZIOKO, Daniel Danladi GAIYA and Idris ABDULLAHI. (2023). Essential secondary metabolites of *Azadirachta indica* leaf in search of drug for COVID-19 treatment: *In-silico* ADMET and bioactivity predictions. *Int. J. Adv. Res. Biol. Sci.* 10(9): 79-93.
DOI: <http://dx.doi.org/10.22192/ijarbs.2023.10.09.010>